COMPREHENSIVE QUANTUM MECHANICAL STUDY ON THE MECHANISTIC, ENERGETIC AND STRUCTURAL PROPERTIES OF ADSORPTION OF DRUG 6-THIOGUANINE ONTO FUNCTIONALIZED CARBON NANOTUBES

M. TEYMOORI, A. MORSALI[*], M. R. BOZORGMEHR,
S. A. BEYRAMABADI
*Department of Chemistry, Mashhad Branch, Islamic Azad University, Mashhad,
Iran & Research Center for Animal Development Applied Biology, Mashhad
Branch, Islamic Azad University, Mashhad 917568, Iran*

Using density functional theory, the six noncovalent interactions and possible mechanisms of covalent functionalization of drug 6-thioguanine with COOH and COCl functionalized carbon nanotube (NTCOOH and NTCOCl) have been investigated. Quantum molecular descriptors of noncovalent configurations were studied. It was specified that binding of drug 6-thioguanine with NTCOOH has more binding energy than NTCOCl and can act as a favorable system for 6-thioguanine drug delivery within biological and chemical systems (noncovalent). NTCOOH and NTCOCl can bond to the amino groups of 6-thioguanine through OH (COOH mechanism) and Cl (COCl mechanism) groups, respectively. The activation energies, the activation enthalpies and the activation Gibbs free energies of six pathways were calculated and compared with each other. The activation parameters related to COOH mechanism are higher than those related to COCl mechanism and therefore COCl mechanism is suitable for covalent functionalization. These results could be generalized to other similar drugs.

1. Introduction

One of the important methods used in the treatment of cancer is through chemotherapy, which is accompanied by different side effects such as vomiting, hair loss, cardio-toxicity and breathing difficulties in the patients. The higher the dose of the anti-cancer drug prescribed, the higher would be the degree of toxicity in the tissues [1,2].

CNTs enjoy unique mechanical, photonic, electronic, and chemical properties [3-8], qualifying them to be used in biological and medical research [9-14].

Due to having properties such as high drug loading capacities and good cell penetration qualities [15], CNTs are more suitable to be used for drug delivery than systems such as polymers, dendrimers, and liposomes, which are being used at present [16,17].

Despite some disadvantages such as low solubility and that they will not be easily discharged from the body, there has been increasing interest during the past two decades for using CNTs in drug delivery [18-22]. Also, the interaction of carbon nanotubes with organic and inorganic molecules has been extensively studied [23-28].

Using CNTs for drug delivery causes reduction in the dosage of the intended drug and consequently the reduction of its side effects [29]. Covalent and noncovalent (hydrogen bonds and van der Waals interactions) functionalizations perform a principle role in the drug delivery systems.

---

*Corresponding author: almorsali@yahoo.com

Thioguanine or 6-thioguanine (TG) belongs to that category of nucleoside drugs which has antitumor, antiviral and anticancer activities and is highly effective in the treatment of acute lymphoblastic leukemia and other tumors [30,31].

Quantum calculations could greatly assist in the design and analysis of drug delivery systems. The granting of Nobel prize for chemistry in 2016 for the design and manufacturing of molecular machines, capable of being used in drug deliverance as well, confirms our statement [32-34].

We have used quantum calculations for analysis of more stable structures and the mechanism of functionalization of the 6-thioguanine drug to CNTs. Such calculations could encourage researchers in manufacturing new drug delivery systems [9,35]. In spite of different theoretical studies on CNTs, so far few studies have been performed on the mechanism of functionalization.

2. Computational details

UB3LYP[36-38] hybrid density functional level and 6-31G(d,p) basis sets in GAUSSIAN 09 package [39] have been used for the optimization of all degrees of freedom for all geometries in solution phase. The solvent play a key role in chemical systems explicitly [40-47] or implicitly. Polarized continuum model (PCM) [48,49] was used for the consideration of implicit effects of the solvent.

The calculations were done on 6-thioguanine, COOH (in water) and COCl (in DMF) functionalized armchair (5,5) SWCNT comprising 114 atoms (10 Å) with the ends terminated by hydrogen atoms. In spite of high computational cost, approximation methods such as ONIOM [50] have not been used.

3. Results and discussion

6-thioguanine (TG) or 2-amino-3,7-dihydropurine-6-thione is a planar molecule with NH_2, NH in six-membered ring and NH in five-membered ring groups as presented in Fig. 1. The optimized geometries of TG, COOH (NTCOOH) and COCl (NTCOCl) functionalized SWCNT in solution phase have been shown in Fig. 1. Use of the functionalized CNTs as well as the drugs having amino groups cause the increase in the solubility of carbon nanotubes.

The interaction between TG and NTCOOH or NTCOCl through amino groups, forms hydrogen bonds. These six reactants (R) have been shown in Figs. 2 and 3, namely, NTCOOH/TG1-3R and NTCOCl/TG1-3R.
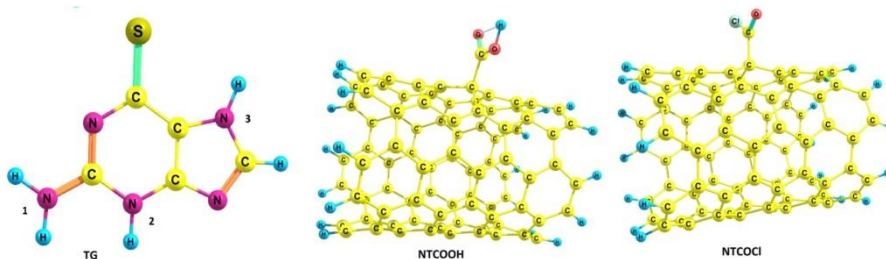

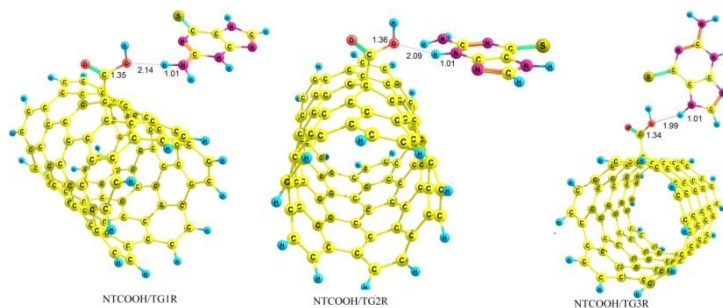Fig. 1. Optimized structures of TG, NTCOOH and NTCOCl.

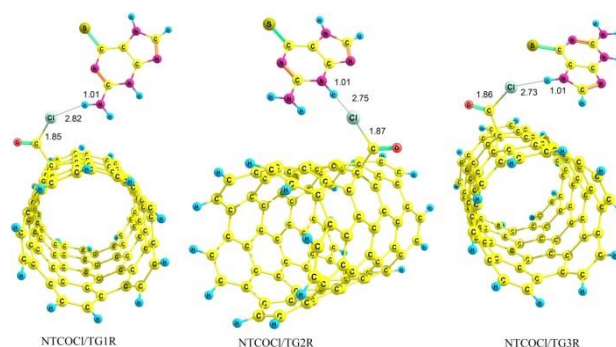Fig. 2. Optimized structures of reactants NTCOOH/TG1-3R

Fig. 3. Optimized structures of reactants NTCOCl/TG1-3R

The binding energies (ΔE) of TG whit NTCOOH (in water) and NTCOCl (in DMF) were calculated using the following equation and presented in Table 1:

$$\Delta E = E_{NTCOOH\,(NTCOCl\,)/TG1-3R} - (E_{NTCOOH\,(NTCOCl\,)} + E_{TG}) \tag{1}$$

Using the calculated binding energies of six configurations in Table 1, these energies are negative in solution phase indicating TG is stabilized by NTCOOH and NTCOCl surfaces. Among the 6 configurations, the configurations related to NTCOOH are more stable than those of NTCOCl configurations. Among the three configurations of NTCOOH/TG1-3R, the third one (NH in five-membered ring) has more negative energy, denoting a stronger interaction. Generally, for noncovalent interactions, comparison between COOH and COCl functionalized single wall carbon nanotube shows that using the first one is more suitable due to a stronger interaction between TG and functionalized SWCNT.

Quantum molecular descriptors such as hardness and electrophilicity index could be used to describe chemical reactivity and stability.

The global hardness (η) indicates the resistance of one molecule against the change in its electronic structure (Eq. 2). Decrease in η causes a decrease in the reactivity and an increase in stability.

$$\eta = (I - A)/2 \tag{2}$$

where $I = -E_{HOMO}$ and $A = -E_{LUMO}$ are the ionization potential and the electron affinity of the molecule, respectively.

Table 1. Quantum molecular descriptors (eV) and binding energies (kJ mol^{-1}) for optimized geometries of TG, NTCOOH (H$_2$O), NTCOCl (DMF), NTCOOH/TG1-3R (H$_2$O) and NTCOCl/TG1-3R (DMF)

Species	E_{HOMO}	E_{LUMO}	E_g	η	μ	ω	ΔE
TG (H$_2$O)	-5.81	-1.56	4.25	2.13	-3.69	3.19	
TG (DMF)	-5.79	-1.55	4.24	2.12	-3.67	3.18	
NTCOOH	-4.04	-2.74	1.30	0.65	-3.39	8.86	
NTCOCl	-4.07	-2.82	1.26	0.63	-3.45	9.46	
NTCOOH/TG1R	-4.06	-2.77	1.29	0.64	-3.42	9.06	-6.52
NTCOOH/TG2R	-4.07	-2.79	1.28	0.64	-3.43	9.16	-13.82
NTCOOH/TG3R	-4.09	-2.84	1.25	0.63	-3.47	9.60	-31.61
NTCOCl/ TG1R	-4.10	-2.86	1.25	0.62	-3.48	9.71	-0.27
NTCOCl/ TG2R	-4.10	-2.86	1.25	0.62	-3.48	9.71	-2.72
NTCOCl/ TG3R	-4.09	-2.84	1.25	0.63	-3.46	9.57	-1.31

Parr defined the electrophilicity index (ω) as follows [51]:

$$\omega = \mu^2 / 2\eta \tag{3}$$

The chemical potential (μ) is defined as follows:

$$\mu = -(I + A) / 2 \tag{4}$$

Table 1 presents the quantum molecular descriptors for TG, NTCOOH (H$_2$O), NTCOCl (DMF), NTCOOH/TG1-3R (H$_2$O) and NTCOCl/TG1-3R (DMF). In this table, E_g (gap of energy between LUMO and HOMO) was also calculated. E_g notably determines a more stable system.

According to the data in Table 1, η and Eg related to the TG drug are higher than those of NTCOOH/TG1-3R and NTCOCl/TG1-3R, showing the stability of TG decreases in the presence of COOH (COCl) functionalized SWCNT and its reactivity increases. Also, it is specified that μ of the TG becomes more positive in the vicinity of NTCOOH and NTCOCl. ω of TG increases in the presence of COOH (COCl) functionalized SWCNT, showing that TG acts as electron acceptor.

For the covalent functionalization, amino groups attack the carbon atom of COOH or COCl to transfer their protons to the OH (Cl) group. We studied these six possible mechanisms for NTCOOH(Cl)/ TG1-3R.

Scheme 1 shows the mechanism for the formation of covalent bond between TG and NTCOOH (COOH mechanism) where k_1 (k_2, k_3) is rate constant and K_1 and K_1' (K_2, K_2', K_3, K_3') are equilibrium constants. In this mechanism, NTCOOH/TG1R(2R,3R) is converted into the product NTCONH and NTCON by losing H$_2$O.
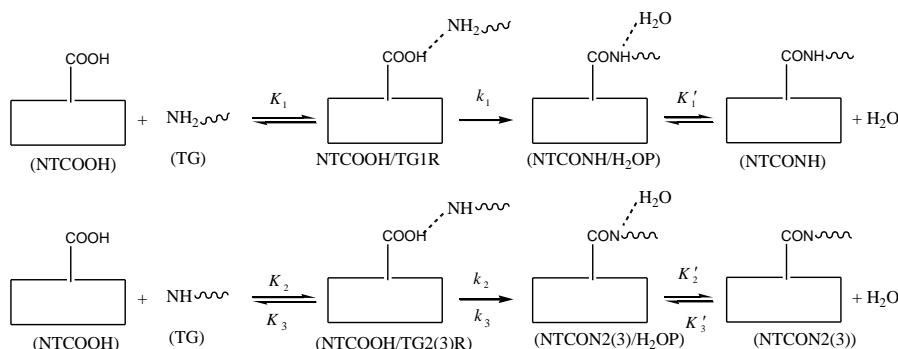
Scheme 1. COOH Mechanism of covalent functionalization

According to the Scheme 1, in COOH mechanism OH from NTCOOH is substituted by NH (N) from TG to give products NTCONH(N2(3)). The optimized structure of products NTCONH(N2(3))/H$_2$OP have been shown in Fig. 4.

Using reactant NTCOOH/TG1R and product NTCONH/H$_2$OP, the transition state of k_1 step was optimized which we call TS$_{k1}$ (Fig. 5). Considering Figs. 2, 4 and 5, the N-H and C-O bond lengths increase (decrease) from 1.01 Å and 1.35 Å (3.63 Å and 4.01 Å) for NTCOOH/TG1R (NTCONH/H$_2$OP) to 2.21 Å and 1.52Å for TS$_{k1}$, respectively.
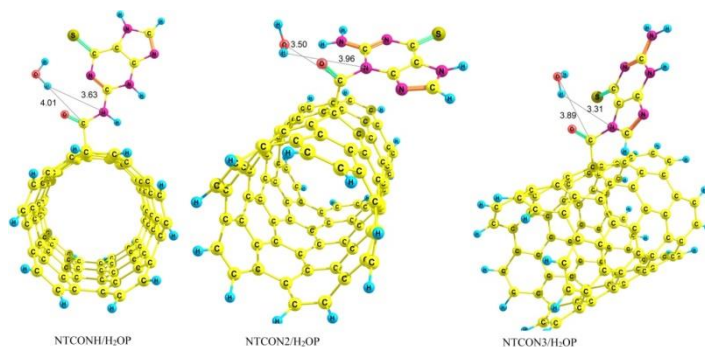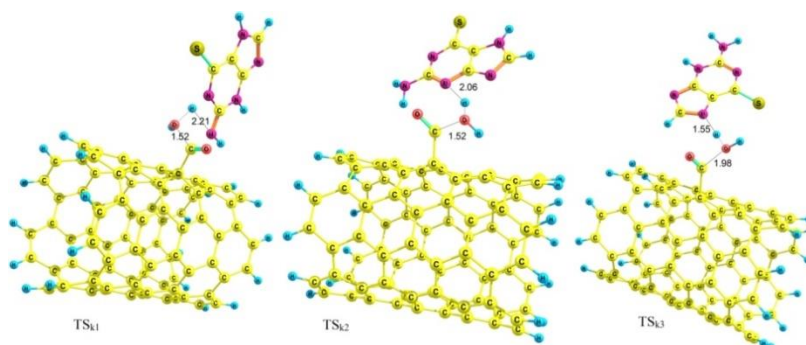

Fig. 4. Optimized structures of products NTCONH(N2(3))/H$_2$OP

Fig. 5. Optimized structures of TS$_{k1}$, TS$_{k2}$ and TS$_{k3}$

Relative energies for optimized structures in all pathways have been calculated in Table 2 by considering electronic plus zero point energy (E), enthalpy (H) and Gibbs free energy (G) of reactants (NTCOOH+TG) equal to zero. The activation energy (E_a), activation enthalpy ($\Delta H^{\ddagger}$) and activation Gibbs free energy ($\Delta G^{\ddagger}$) for k_1 step are 181.90 kJ mol^{-1}, 187.68 kJ mol^{-1} and 190.49 kJ mol^{-1}, respectively (Table 2). The total rate constant for overall reaction (COOH/NH pathway) is equal to $k_1 \times K_1$, so the total activation energy ($E_a(\text{COOH}/\text{NH}) = E_a(k_1\text{step}) + \Delta E(K_1\text{step})$), the total activation enthalpy ($\Delta H^{\ddagger}(\text{COOH}/\text{NH}) = \Delta H^{\ddagger}(k_1\text{step}) + \Delta H(K_1\text{step})$) and total activation Gibbs free energy ($\Delta G^{\ddagger}(\text{COOH}/\text{NH}) = \Delta G^{\ddagger}(k_1\text{step}) + \Delta G(K_1\text{step})$) for COOH/TG1 mechanism are 175.38 kJ mol^{-1}, 188.37 kJ mol^{-1} and 219.62 kJ mol^{-1}, respectively (Table 2).

Table 2. Relative energies (kJ mol^{-1}) for different species in COOH and COCl mechanisms. E, H and G are electronic plus zero point energy, enthalpy and Gibbs free energy, respectively

| species	E	H	G
In water	COOH mechanism		
NTCOOH+TG	0.00	0.00	0.00
NTCOOH/TG1R	-6.52	0.69	29.13
TS$_{k1}$	175.38	188.37	219.62
NTCONH/H$_2$OP	20.29	27.97	60.53
NTCOOH/TG2R	-13.82	-7.05	24.88
TS$_{k2}$	185.27	192.86	227.49
NTCOON2/H$_2$OP	78.30	86.64	123.38
NTCOOH/TG3R	-31.61	-27.79	15.76
TS$_{k3}$	204.78	218.94	251.10
NTCON2/H$_2$OP	80.60	90.30	124.09
In DMF	COCl mehanism		
NTCOCl+TG	0.00	0.00	0.00
NTCOCl/TG1R	-0.27	7.25	32.57
TS$_{k4}$	60.82	71.52	99.78
NTCONH/HClP	-34.91	-22.90	8.63
NTCOCl/TG2R	-2.72	4.86	31.99
TS$_{k5}$	110.11	124.84	152.24
NTCON2/HClP	33.65	40.73	75.95
NTCOCl/TG3R	-1.31	6.35	30.99
TS$_{k6}$	137.76	147.33	186.37
NTCON3/HClP	21.23	29.40	64.57

Similar to k_1 step, using NTCOOH/TG2R (NTCOOH/TG3R) and NTCON2/H$_2$OP (NTCON3/H$_2$OP), the transition state of k_2 (k_3) step (Figure 5) was obtained which we call TS$_{k2}$ (TS$_{k3}$). Considering Figs. 2, 4 and 5, the N-H and C-O bond lengths increase from 1.01 Å and 1.36 Å (1.01 Å and 1.34 Å) for NTCOOH/TG2R (NTCOOH/TG3R) and decrease from 3.96 Å and 3.50 Å (3.31 Å and 3.89 Å) for NTCON2/H$_2$OP (NTCON3/H$_2$OP) to 2.06 Å and 1.52Å (1.55 and 1.98) for TS$_{k2}$ (TS$_{k3}$), respectively.

E_a, $\Delta H^{\ddagger}$ and $\Delta G^{\ddagger}$ for k_2 (k_3) step are 199.09 kJ mol^{-1}, 199.91 kJ mol^{-1} and 202.61 kJ mol^{-1} (236.39 kJ mol^{-1}, 246.73 kJ mol^{-1} and 235.34 kJ mol^{-1}), respectively (Table 2). Using equations similar to the ones given for COOH/TG1 mechanism, the total activation energy, the total activation enthalpy and the total activation Gibbs free energy for COOH/TG2 (COOH/TG3) mechanism are 185.27 kJ mol^{-1}, 192.86 kJ mol^{-1} and 227.49 kJ mol^{-1} (204.78 kJ mol^{-1}, 218.94 kJ mol^{-1} and 251.10 kJ mol^{-1}), respectively (Table 2). In room temperature, the energy barriers related to COOH mechanism are too high to occur.

The other reactions for the covalent functionalization of TG onto COCl functionalized carbon nanotube are shown in Scheme 2 (COCl mechanism) [52]. In these reactions, NTCOOH was firstly converted into alkyl chloride using SOCl$_2$ (NTCOCl). TG then reacts with NTCOCl to form covalent bond.

COCl mechanism begins with the attack of amino groups of TG to Cl in the NTCOCl to form products NTCONH(N2(3))/HClP (Fig. 6).

Using NTCOCl/TG1R and NTCONH/HClP, a transition state is optimized which we call TS$_{k4}$ (Fig. 7). Considering Figs. 3, 6 and 7, the C-Cl and N-H bond lengths increase (decrease) from 1.85 Å and 1.01 Å (4.05 Å and 3.96 Å) for NTCOCl/TG1R (NTCONH/HClP) to 3.89 Å and 1.05 Å for TS$_{k4}$, respectively. E_a, $\Delta H^{\ddagger}$ and $\Delta G^{\ddagger}$ for k_4 step are 61.09 kJ mol^{-1}, 64.27 kJ mol^{-1} and 67.21 kJ mol^{-1}, respectively (Table 2). the total activation energy, the total activation enthalpy and the total activation Gibbs free energy for COCl/TG1 mechanism are 60.82 kJ mol^{-1}, 71.52 kJ mol^{-1} and 99.78 kJ mol^{-1}, respectively (Table 2).
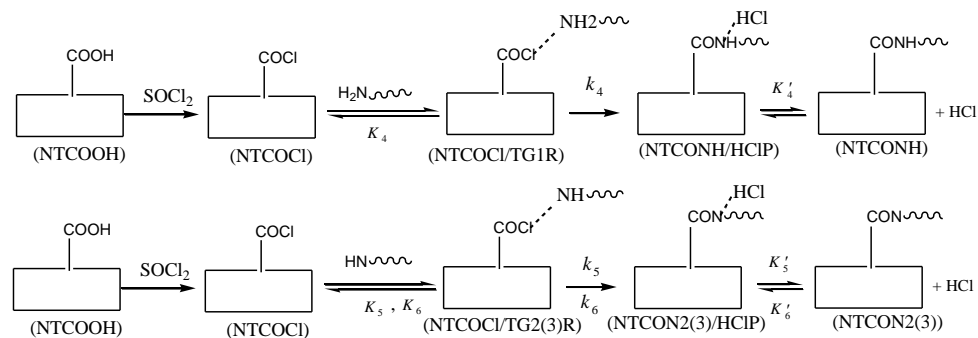
Scheme 2. COCl Mechanism of covalent functionalization

Using reactants NTCOCl/TG2R and NTCOCl/TG3R and products NTCON2/HClP and NTCON3/HClP, the transition states of k_5 and k_6 step were obtained which we call TS_{k5} and TS_{k6}, respectively (Fig. 7). Considering Figs. 3, 6 and 7, the N-H and C-Cl bond lengths increase from 1.01 Å and 1.87 Å (1.01 Å and 1.86 Å) for NTCOCl/TG2R (NTCOCl/TG3R) and decrease from 3.10 Å and 4.06 Å (3.12 Å and 4.02 Å) for NTCON2/HClP (NTCON3/HClP) to 1.12 Å and 2.34 Å (1.54 and 3.06) for TS_{k5} (TS_{k6}), respectively.
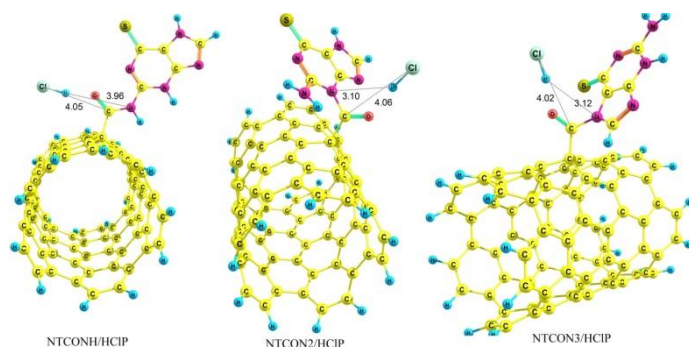

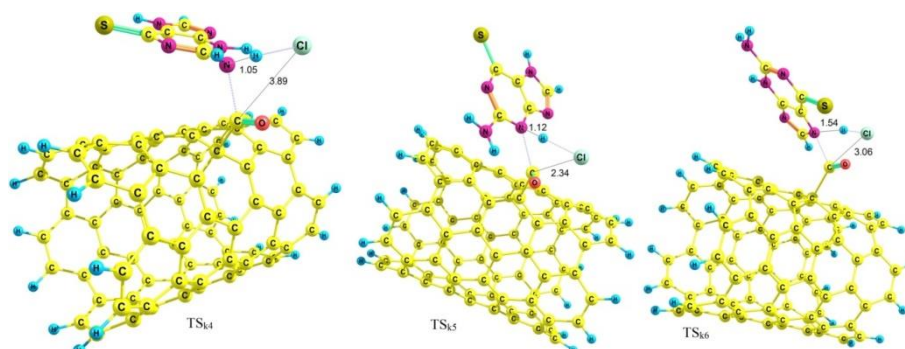*Fig. 6. Optimized structures of products NTCONH(N2(3))/HCl*

Fig. 7. Optimized structures of TS_{k4}, TS_{k5} and TS_{k6}

E_a, $\Delta H^{\ddagger}$ and $\Delta G^{\ddagger}$ for k_5 (k_6) step are 112.83 kJ mol^{-1}, 119.98 kJ mol^{-1} and 120.25 kJ mol^{-1} (139.07 kJ mol^{-1}, 140.98 kJ mol^{-1} and 155.38 kJ mol^{-1}), respectively (Table 2). The total activation energy, the total activation enthalpy and the total activation Gibbs free energy for COCl/TG2 (COCl/TG3) mechanism are 110.11 kJ mol^{-1}, 124.84 kJ mol^{-1} and 152.24 kJ mol^{-1} (137.76 kJ mol^{-1}, 147.33 kJ mol^{-1} and 186.37 kJ mol^{-1}), respectively (Table 2).

The total activation energies for COCl/TG1-3 mechanisms are lower than COOH/TG1-3 mechanisms by 114.56 kJ mol^{-1}, 75.16 kJ mol^{-1} and 67.02 kJ mol^{-1}, respectively. Amongst COCl/TG1-3 mechanisms, the contribution of COCl/TG1 (from NH$_2$) mechanism is higher.

Both mechanisms (COOH and COCl) are nucleophilic substitution reactions. Generally these reactions proceed through a tetrahedral intermediate. We designed a tetrahedral intermediate as input and ultimately a structure was optimized which is similar to reactant NTCOCl/TG. This means that tetrahedral intermediate could not be existed, being probably due to electronic and steric effects carbon nanotubes.

4. Conclusions

Six possible configurations of noncovalent interaction of drug 6-thioguanine (TG) onto NTCOOH and NTCOCl were studied. The binding energies related to NTCOCl are lower than those related to NTCOOH, indicating NTCOOH/TG configurations are stabilized. The global hardness and HOMO-LUMO energy gap of NTCOOH/TG configurations are higher than those of NTCOCl/TG configurations, showing the reactivity of the 6-thioguanine increases in the presence of NTCOCl and its stability decreases.

Two mechanisms of covalent functionalization of drug 6-thioguanine onto NTCOOH (COOH mechanism) and NTCOCl (COCl mechanism) have been investigated in detail. Each mechanism involves three pathways, because 6-thioguanine can bond to NTCOOH or NTCOCl through amino groups. The activation parameters related to COOH mechanisms are higher than those related to COCl mechanisms. The lowest activation energy is related to COCl/TG1 pathway. In this mechanism 6-thioguanine is bonded to NTCOCl via NH$_2$ group.

Acknowledgments

References

[1] G. D. Pennock, W. S. Dalton, W. R. Roeske, C. P. Appleton, K. Mosley, P. Plezia, T. P. Miller, S. E. Salmon, J. Natl. Cancer Inst. **83**, 105 (1991).
[2] C. Lindley, J. S. McCune, T. E. Thomason, D. Lauder, A. Sauls, S. Adkins, W. T. Sawyer, Cancer pract. **7**, 59 (1999).
[3] P. Lai, S. Chen, M.-F. Lin, Physica E **40**, 2056 (2008).
[4] M. F. De Volder, S. H. Tawfick, R. H. Baughman, A. J. Hart, Science **339**, 535 (2013).
[5] S.-J. Sun, J. W. Fan, C.-Y. Lin, Physica E **44**, 803 (2012).
[6] U. N. Maiti, W. J. Lee, J. M. Lee, Y. Oh, J. Y. Kim, J. E. Kim, J. Shim, T. H. Han, S. O. Kim, Adv. Mater. **26**, 40 (2014).
[7] I. Baltog, M. Baibarac, L. Mihut, S. Lefrant, Dig. J. Nanomater. Biostruct. **2**, 185 (2007).
[8] E. Vajaiac, S. Palade, A. Pantazi, A. Stefan, G. Pelin, D. Baran, C. Ban, M. Purica, V. Meltzer, E. Pincu, Dig. J. Nanomater. Biostruct. **10** (2015).
[9] C. Rungnim, U. Arsawang, T. Rungrotmongkol, S. Hannongbua, Chem. Phys. Lett. **550**, 99 (2012).
[10] S. P. Zhang, L. G. Shan, Z. R. Tian, Y. Zheng, L. Y. Shi, D. S. Zhang, Chin. Chem. Lett. **19**, 592 (2008).
[11] M. Adeli, R. Soleyman, Z. Beiranvand, F. Madani, Chem. Soc. Rev. **42**, 5231 (2013).
[12] R. V. Mundra, X. Wu, J. Sauer, J. S. Dordick, R. S. Kane, Curr. Opin. Biotechnol. **28**, 25 (2014).
[13] A. Li, L. Wang, M. Li, Z. Xu, P. Li, Z. Zhang, Dig. J. Nanomater. Biostruct. **9**, 59 (2014).
[14] T. Mocan, S. Clichici, A. Biris, S. Simon, C. Catoi, F. Tabaran, A. Filip, D. Daicoviciu, N. Decea, R. Moldovan, Dig. J. Nanomater. Biostruct. **6**, 1207 (2011).

[15] M. Prato, K. Kostarelos, A. Bianco, Acc. Chem. Res. **41**, 60 (2007).

[16] T. M. Allen, P. R. Cullis, Science **303**, 1818 (2004).

[17] D. Tomalia, L. Reyna, S. Svenson, Biochem. Soc. Trans. **35**, 61 (2007).

[18] H. Zhang, L. Hou, X. Jiao, Y. Ji, X. Zhu, H. Li, X. Chen, J. Ren, Y. Xia, Z. Zhang, Curr. Pharm. Biotechnol. **14**, 1105 (2014).

[19] S. Unnati, R. Shah, Int. J. Pharm. Technol. **3**, 927 (2011).

[20] C. Ciobotaru, C. Damian, S. Polosan, M. Prodana, H. Iovu, Dig. J. Nanomater. Biostruct. **9**, 859 (2014).

[21] B. S. Wong, S. L. Yoong, A. Jagusiak, T. Panczyk, H. K. Ho, W. H. Ang, G. Pastorin, Adv. Drug Deliv. Rev. **65**, 1964 (2013).

[22] C. C. Ciobotaru, M. C. Damian, S. Polosan, E. Matei, H. Iovu, Dig. J. Nanomater. Biostruct. **9**, 413 (2014).

[23] Y. Lin, L. F. Allard, Y.-P. Sun, J. Phys. Chem. B **108**, 3760 (2004).

[24] C. M. Chang, H. L. Tseng, A. de Leon, A. Posada-Amarillas, A. F. Jalbout, J. Comput. Theor. Nanosci. **10**, 521 (2013).

[25] S. A. Tawfik, S. El-Sheikh, N. Salem, Physica E **44**, 111 (2011).

[26] B. Soleimani, S. Rostamnia, A. Ahmadi, Digest J. of Nanom. and Biostruct **5**, 153 (2010).

[27] A. Osikoya, D. Wankasi, R. Vala, A. Afolabi, E. Dikio, Dig. J. Nanomater. Biostruct. **9**, 1187 (2014).

[28] A. Osikoya, D. Wankasi, R. Vala, C. Dikio, A. Afolabi, N. Ayawei, E. Dikio, Dig. J. Nanomater. Biostruct. **10** (2015).

[29] K. Ajima, M. Yudasaka, T. Murakami, A. Maigné, K. Shiba, S. Iijima, Mol. pharm. **2**, 475 (2005).

[30] G. LePage, Cancer Res. **23**, 1202 (1963).

[31] B. F. Pan, J. A. Nelson, Biochem. Pharmacol. **40**, 1063 (1990).

[32] Y. B. Zheng, B. Kiraly, T. J. Huang, Nanomedicine **5**, 1309 (2010).

[33] V. Linko, A. Ora, M. A. Kostiainen, Trends Biotechnol. **33**, 586 (2015).

[34] W. Szymański, J. M. Beierle, H. A. Kistemaker, W. A. Velema, B. L. Feringa, Chem. Rev. **113**, 6114 (2013).

[35] C. Rungnim, T. Rungrotmongkol, S. Hannongbua, H. Okumura, J. Mol. Graphics Modell. **39**, 183 (2013).

[36] A. D. Becke, Phys. Rev. A **38**, 3098 (1988).

[37] A. D. Becke, J. Chem. Phys. **98**, 5648 (1993).

[38] C. Lee, W. Yang, R. G. Parr, Phys. Rev. B **37**, 785 (1988).

[39] M. Frisch, G. Trucks, H. Schlegel, G. Scuseria, M. Robb, J. Cheeseman, G. Scalmani, V. Barone, B. Mennucci, G. Petersson, Wallingford, CT (2009).

[40] S. Hooman Vahidi, A. Morsali, S. Ali Beyramabadi, Comp. Theor. Chem. **994**, 41 (2012).

[41] A. Akbari, F. Hoseinzade, A. Morsali, S. A. Beyramabadi, Inorg. Chim. Acta **394**, 423 (2013).

[42] A. Morsali, F. Hoseinzade, A. Akbari, S. A. Beyramabadi, R. Ghiasi, J. Solution Chem. **42**, 1902 (2013).

[43] S. Mohseni, M. Bakavoli, A. Morsali, Prog. React. Kinet. Mec. **39**, 89 (2014).

[44] S. A. Beyramabadi, H. Eshtiagh-Hosseini, M. R. Housaindokht, A. Morsali, Organometallics **27**, 72 (2007).

[45] A. Gharib, A. Morsali, S. Beyramabadi, H. Chegini, M. N. Ardabili, Prog. React. Kinet. Mec. **39**, 354 (2014).

[46] A. Morsali, Int. J. Chem. Kinet. **47**, 73 (2015).

[47] M. N. Ardabili, A. Morsali, S. A. Beyramabadi, H. Chegini, A. Gharib, Res. Chem. Intermed. **41**, 5389 (2015).

[48] R. Cammi, J. Tomasi, J. Comput. Chem. **16**, 1449 (1995).

[49] J. Tomasi, M. Persico, Chem. Rev. **94**, 2027 (1994).

[50] S. Dapprich, I. Komáromi, K. S. Byun, K. Morokuma, M. J. Frisch, J. Mol. Struc.: THEOCHEM **461**, 1 (1999).

[51] R. G. Parr, L. v. Szentpaly, S. Liu, J. Am. Chem. Soc. **121**, 1922 (1999).

[52] T. Lin, V. Bajpai, T. Ji, L. Dai, Aust. J. Chem. **56**, 635 (2003).